CDR Project Year–1 Annual Report

Enabling Consistent Calibration of Multispectral Solar Reflective Imager Data for Climate Data Record Development Using the Moon

Thomas C. Stone — PI
U.S. Geological Survey, Flagstaff, AZ

15 July, 2012

1 Introduction and Background

The overall objective of this project is to provide an independent assessment of radiometric calibration for visible-wavelength imagers on meteorological satellites, to support development of the data products from these instruments into Climate Data Records (CDRs). The lunar calibration technique applied here utilizes the Moon as a radiometric reference for the instruments that have viewed it. To accommodate the constantly varying brightness of the Moon through its phases (among other effects), the lunar reference consists of an analytic numerical model. This model, developed at the USGS Flagstaff Science Center, predicts the lunar spectral irradiance at reflective solar wavelengths, outside the atmosphere, for the particular viewing circumstances of a sensor in Earth orbit. The results can effectively normalize the variations in lunar brightness for the different instrument observations with sub-percent precision, thus providing a stable radiometric reference.

The Moon periodically appears in the view field of space-based meteorological imagers, either in the corners and margins of the rectangular field of regard (FOR) of geostationary imagers, as shown in Figure 1, or in the space view (SV) sector of polar orbiting cross-track scanners such as the Advanced Very High Resolution Radiometer (AVHRR). Finding lunar images in the archives of meteorological satellite data involves predicting the relative geometries of the Moon, the spacecraft, and the orientation of the imager view field. Identifying satellite images containing the Moon and obtaining the archived data for use in this study was the first task of this CDR project.

Applying lunar calibration techniques to satellite imaging instruments involves measurement of the spatially integrated lunar irradiance from images of the Moon. These measurements provide an evaluation of the radiometric response of the imager sensors at the time of each lunar observation. Taken as a series, the measurements reveal sensor response trends over time, after application of the lunar model results to normalize the brightness of the Moon for each observation. Temporal trending is quantified by fitting some form of degradation function of time, leading to a calibration stability measurement and correction for the instrument. These results are then usable for cross-comparisons to develop an assessment of the calibration biases between the sensors, regardless of whether the instruments overlap in their operational periods. The level of precision potentially achievable for these calibration evaluations demonstrates their utility for the development of CDRs.

The current project accomplishments toward meeting these objectives are detailed in this report. The satellites used in this study to date include GOES–8 through 13, Meteosat Second Generation (MSG) 1 and 2 (Meteosat–8 and 9), and NOAA–16.

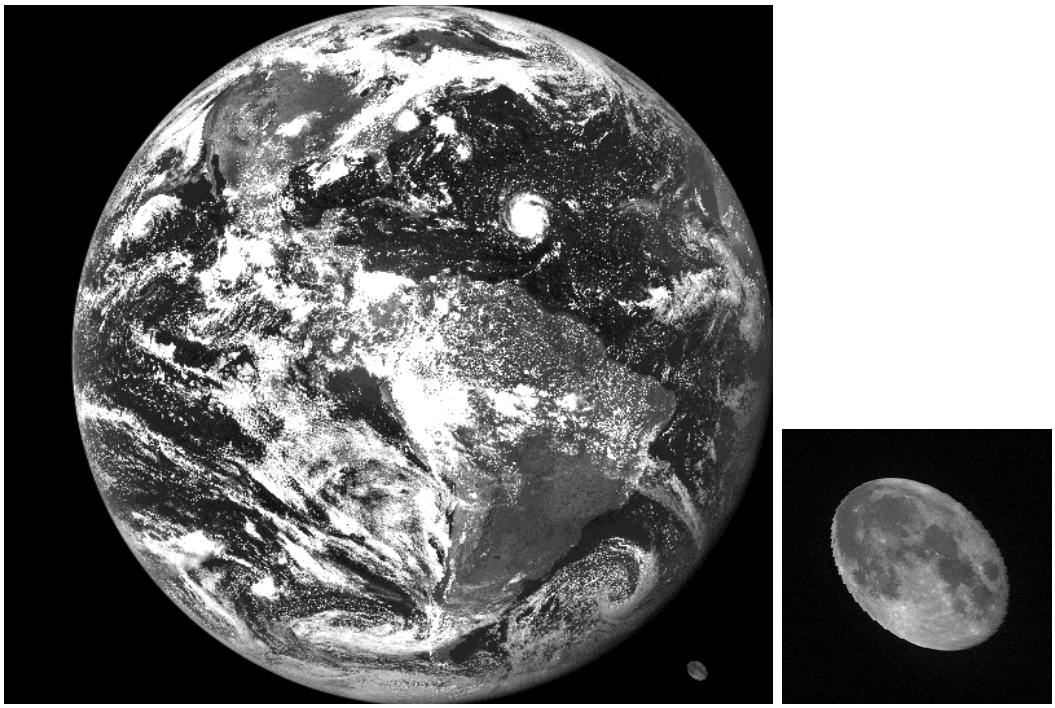

Figure 1: GOES–12 Full Disk image acquired 2004-08-30 17:45:14 that captured the Moon, shown enlarged (right). The lunar disk image appears skewed due to the apparent motion of the Moon across the view field during the image acquisition time, actually caused by the satellite orbital motion.

2 Lunar Image Data Acquisition

In 2005 NOAA implemented routine space looks that targeted the Moon with the GOES–East and West satellites. These data were utilized here, in addition to the larger number of Moon images that were acquired by chance, i.e. by fortuitous coincidence of the Moon being in the view field during routine imaging. Images in the archives of meteorological satellite data that potentially captured the Moon were identified by numerical prediction of coincident view geometries, based on the relative positions of the satellites and the Moon, and consideration of the sensor look direction.

For the satellites used in this study, the spacecraft positions at particular times were computed by propagating the satellite orbit from two-line orbital element (TLE) sets obtained from Space-Track (`www.space-track.org`), using SGP4 software implemented in IDL. The position of the Moon was computed using the DE421 double-precision ephemeris software, also in an IDL implementation. These two programs generate Earth-centered inertial coordinates in the J2000 system.

The software routine used here to find coincidental Moon images accepts as input the operational imaging schedules of the geostationary satellites. Times found to have favorable view geometries were passed to a further routine that simulates the imager scanning sequence. Full Disk, and sector coverages for Northern Hemisphere, CONUS/PACUS, and Southern Hemisphere were simulated for the GOES satellites. Only Full Disk imaging simulations were required for the Spinning Enhanced Visible and Infrared Imager (SEVIRI) instruments on MSG, as this is its normal operating mode. To account for inaccuracies in the spacecraft positions determined from the orbit propagations, tolerances were expanded for triggering indications of the Moon in the view field, leading to an

increased number of "false positive" predictions that had to be culled.

The data files potentially containing Moon images were ordered and downloaded in raw format from the archive servers — NOAA's Comprehensive Large Array-data Stewardship System (CLASS) for GOES and AVHRR, and the EUMETSAT Data Centre for SEVIRI. Because the location of the lunar disk within image frames cannot be predicted with high accuracy due to spacecraft position and attitude uncertainties, each visible channel image was viewed interactively, and those with Moon captures were saved out for lunar calibration analysis. In addition, the GOES space-look data for the dedicated observations of the Moon were identified and ordered from CLASS for GOES–10 through 13. Table 1 lists the geostationary satellites used in this study to date, with the dates for earliest and latest usable Moon images found and the number of images used. Refinements to the Moon appearance prediction routines may add to these numbers.

Table 1: Inclusive dates for geostationary images usable for lunar calibration analysis

Satellite	First Date	Last Date	Number of Moon Images
GOES–8	1995–01–08	2003–02–20	44
GOES–9	1995–12–12	1998–04–12	9
GOES–10	1998–08–09	2006–06–06	49
GOES–11	2006–09–08	2011–12–04	77
GOES–12	2003–04–14	2010–03–02	49
GOES–13	2010–07–30	2012–05–31	26
MSG–1	2004–02–09	2005–12–08	36
MSG–2	2006–08–13	2009–02–10	49

For the AVHRR instruments on NOAA polar orbiting spacecraft, the process for predicting Moon appearances is similar, with the exception that the sensor look direction (in space view) is tied to the spacecraft velocity vector. The SGP4 orbit propagator provides the satellite state vector, which includes the velocity components. The current project work has examined AVHRR imagery for a sample set of NOAA–16 GAC data, where the presence of the Moon was known *a priori*. Details of this analysis are given in §5 below.

3 Moon Image Processing and Lunar Calibration Analysis — Discussion

The USGS lunar calibration system operates with the radiometric quantity of spatially integrated lunar spectral irradiance. Measurements from images of the Moon acquired by spacecraft instruments are compared against computations of the lunar irradiance model, where the model results are generated for the particular conditions of the instrument observations, including the instrument spectral response. An overview discussion of procedures is presented here, with the results for each satellite following in §4.

3.1 Lunar Irradiance Measurements from Images

Processing of lunar image data to irradiance (E) involves summation of pixels that make up the Moon's disk. Raw pixel values in digital Data Numbers (DN) are dark-corrected and converted to

radiance (L), and the irradiance summation is given by:

$$E = \Omega_{\text{pix}} \sum_{i=1}^{N} L_i \tag{1}$$

where Ω_{pix} is the solid angle subtended by one pixel, L_i is the radiance measure of pixel i, and the summation covers all pixels on the lunar disk N. Pixel solid angles are computed from the native spatial resolution of each imager, found in technical datasheets. The summation includes any spatial oversampling associated with the image acquisition; this must be accounted for in the downstream processing for comparison with model results.

To facilitate the irradiance measurements, subframes containing the Moon and a sampling of surrounding space were extracted from the full-frame Earth image data. This extraction is by necessity an interactive process, to contend with proximities to the image frame edges and the bright Earth disk. Selection of pixels designated as on the lunar disk utilizes a threshold test applied to the subframe pixel brightness level, accepting pixels that exceed a specified threshold above the dark (space view) level, and also including pixels within a specified spatial proximity to the above-threshold pixels. Figure 2 shows the extracted subframe for the GOES–12 image of Figure 1, and the corresponding on-Moon pixel selection mask. This display has retained the native East-West oversampling (a factor of 1.75), thus giving the elongated appearance. The sawtooth edge pattern results from the image construction of sequential scan lines, having 8 pixels (detectors) in each line, and where the orbital motion of the satellite over the duration of each scan induces a horizontal offset in the apparent position of the Moon for each line.

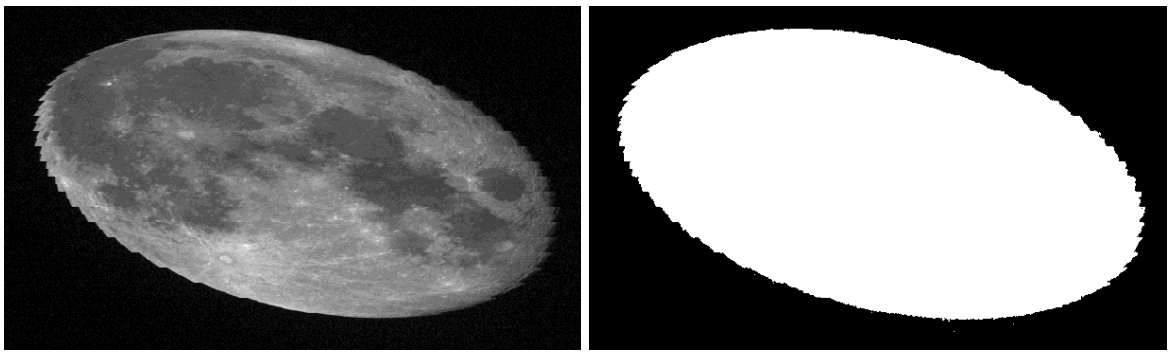

Figure 2: Subframe containing the Moon extracted from GOES–12 Full Disk image acquired 2004–08–30 17:45:14, and the corresponding on-Moon pixel selection mask.

Conversion of the raw pixel values in DN, or counts, to radiance utilized the pre-launch calibration coefficients for each satellite, obtained from online documentation provided by the satellite operators (NOAA and EUMETSAT). Using constant coefficients enables characterization of the sensor response trends over time. Only the calibration slope values (related to sensor gain) were used here, while the sensor response to zero radiance (related to the calibration intercept) was evaluated for each image individually from analysis of the space-viewing pixels surrounding the Moon.

3.2 Lunar Model Outputs and Comparison Against Measurements

In operation, the USGS lunar irradiance model generates the spatially integrated reflectance of the Moon's disk in a 32-wavelength discrete spectrum. The lunar disk reflectance is governed only

by geometry, specifically the phase angle and the particular hemispheres of the Moon that are illuminated and viewed (these define the lunar librations). The normal inputs to the USGS system are the time of observation, and the instrument (i.e. spacecraft) location in Earth-centered inertial coordinates at the observation time. A one-time setup for the instrument spectral response is a prerequisite. The model system computes a planetary ephemeris to obtain the positions of the Sun and Moon, from which the actual geometry inputs for the numerical reflectance model (the phase and librations) are computed. These reflectance values are interpolated to the instrument band wavelengths along a representative spectrum before being converted to irradiance. For wide-band sensors such as the GOES visible channels, a weighted sampling of the 32 model wavelengths is used.

The lunar irradiance measured by an instrument has $1/r^2$ dependencies on the Sun–Moon and Moon-observer distances. The irradiance model results at the instrument wavelengths are corrected to the actual distances of the observations, and scaled to account for any oversampling incurred during image acquisition. The final, corrected outputs are directly comparable to the measurements from images.

3.3 Sensor Response Trending and Instrument Cross-comparison

The results from the lunar calibration analysis are expressed here as the ratio of irradiance measurements to model outputs. This effectively normalizes the varying brightness of the Moon with the individual observations. Collecting these results into time series for each satellite enables quantitative evaluation of changes in the sensor response over time. This is typically done by fitting an analytic function of time to the series results, thus providing a time-dependent correction for the sensor response which can be used to stabilize the instrument calibration. Sub-percent precision has been achieved with this method for instruments that have viewed the Moon a large number of times. Applying this type of trend analysis to the imagers used in this study has enabled comparison to the post-launch operational calibration corrections published by the satellite operators.

With application of the temporal calibration corrections, the lunar time series for each satellite become distributions of normalized measurements of an external, stable standard — the Moon. The statistical means of these distributions form the basis for cross-comparison between instruments, thus providing inter-instrument bias measurements with quantifiable uncertainties. Developing these bias comparisons is the current focus of efforts of this CDR project.

4 Results for Geostationary Satellites

4.1 GOES

Most of the routine imaging spatial sectors for GOES visible channels have a portion that views deep space, although this can be quite small in some cases (e.g. CONUS/PACUS). The Moon appearance prediction algorithm described above (§2) accounts for the routine imaging schedules and the spatial boundaries of the various sectors for simulating the scan sequences and finding coincidences with the Moon. This was done for the Northern Hemisphere, CONUS/PACUS, and Southern Hemisphere sectors, as well as Full Disk imaging. Refinements to the appearance prediction program have focused on assuring that all Moon captures are found. An expected effect of this is that a number of the positive predictions are for images where the lunar disk is partially clipped, either by the Earth of the frame edge. It turns out GOES–9 has an unusually high incidence of clipped images.

The plots on the following page show comparisons of measured to modeled lunar irradiances,

given as simple ratios, for the usable data to date for GOES–8 through GOES–13. For the pre-GVAR satellites (earlier than GOES–8), the different image acquisition method requires different procedures for the Moon appearance predictions, and there are very few holdings in CLASS for these satellites, leading to a search for alternate ways to obtain image data. Consequently, results for GOES–5 through 7 are not presented here.

The time series for each GOES imager have been fitted with an analytic function of time, shown as solid lines in the plots. The inverse of these functions provides a calibration correction for the sensors. For the GOES imagers, a type of exponential decay was found to model the sensor response trends adequately. This function has the form:

$$E_{\text{meas}}/E_{\text{model}} = a_0 + a_1 \left[1. - \exp\left(-a_2(t - t_0)\right)\right] \tag{2}$$

where $(t - t_0)$ is the time difference in days from the series start time t_0. The start times were chosen to coincide with the calibration trend analysis published by NOAA–NESDIS–STAR at:
`http://www.star.nesdis.noaa.gov/smcd/spb/fwu/homepage/GOES_Imager_Vis_Cal.php`
Table 2 gives the parameters for Equation 2, where the coefficients a_n were found by non-linear least-squares fitting of the irradiance ratio data. For GOES–11, a linear polynomial $a_0 + a_1(t - t_0)$ was found to fit the observed trend better than Equation 2, and the corresponding parameters are given in the table.

Table 2: Sensor response trend analysis results

Satellite	Series Start Date (t_0)	Fit Parameters		
		a_0	a_1	a_2
GOES–8	1995–04–10	0.7860	-0.4663	2.235e-4
GOES–9	1995–08–07	1.024	-0.1448	5.951e-3
GOES–10	1998–03–21	1.068	-0.4268	7.108e-4
GOES–11	2006–06–21	0.9317	-8.592e-5	linear
GOES–12	2003–04–01	0.9648	-0.2810	6.276e-4
GOES–13	2010–04–14	0.9511	-0.1306	2.025e-3

Taking the inverse of these fitted trend functions provides temporal calibration corrections that can be applied directly to radiance data products from the instruments. The operational post-launch calibration for GOES visible channel imagers developed by NOAA–NESDIS–STAR is based on a cross-calibration approach, using NASA's Moderate Resolution Imaging Spectroradiometer (MODIS) as the standard. Calibration correction factors for GOES–11, 12, 13, and 15 have been published by NOAA at:
`http://www.star.nesdis.noaa.gov/smcd/spb/fwu/homepage/GOES_Imager_Vis_OpCal.php`
Figure 4 shows comparisons of the NOAA-derived correction factors (open symbols) with those derived from the current lunar work (filled symbols). The times specified for these data points have been taken as the 15th day of the month following the "Coefficient Generation Month" in the NOAA listings. The lunar-based analytic functions were evaluated for these same times. Since both sets of corrections were generated by comparisons against radiometric standards (MODIS measurements of ground targets, and the Moon), the offsets between the two methods are not artifacts, but represent real systematic errors.

4.2 SEVIRI

The Spinning Enhanced Visible and Infrared Imager (SEVIRI) is a spin-scan imaging system that acquires Full Disk images on a 15-minute repeat cycle. This simplifies the Moon appearance

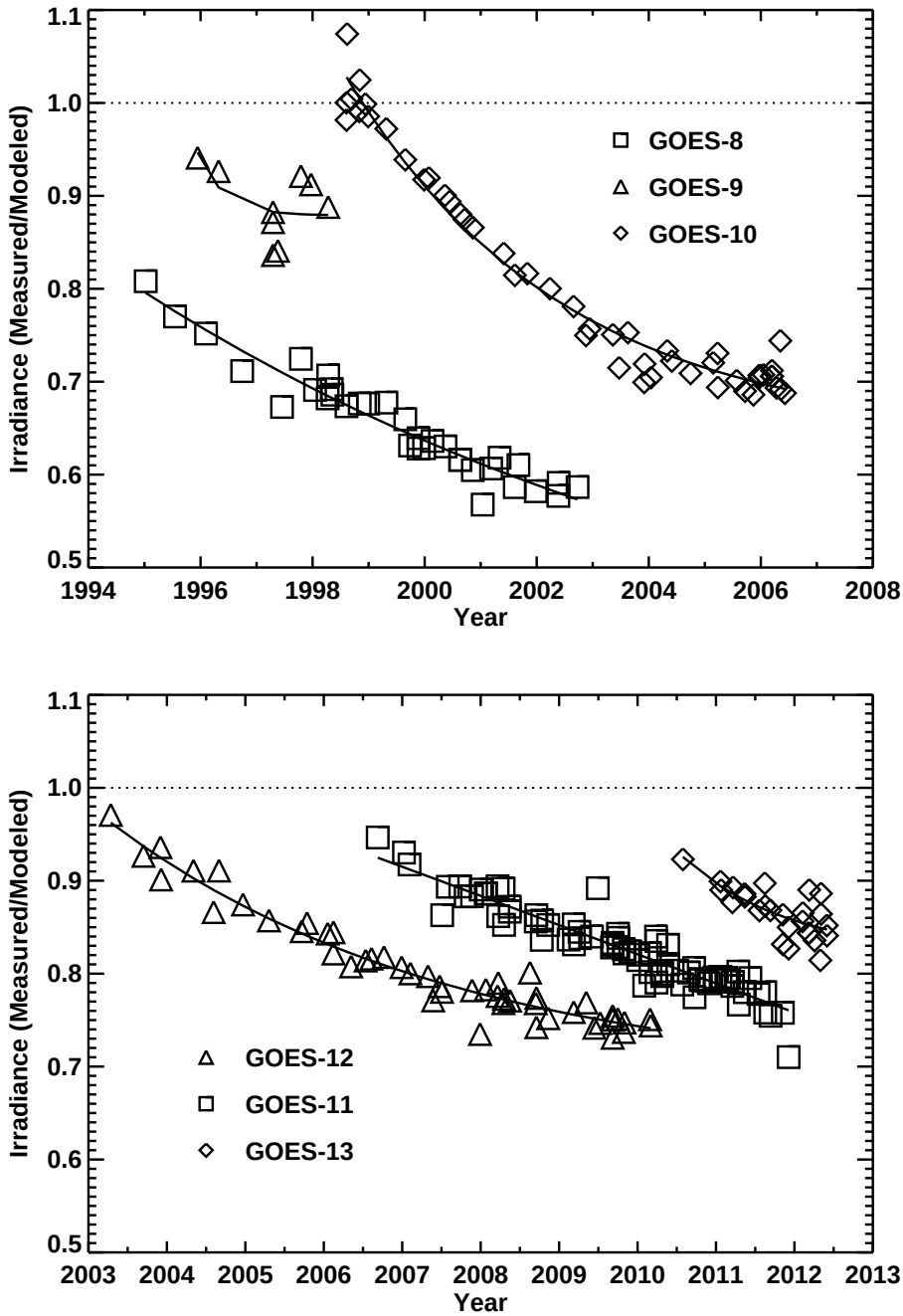

Figure 3: Time series of lunar calibration results for GOES–8 through GOES–13, given as ratios of measured lunar irradiance to USGS model outputs. Fitted trend analysis results are shown as solid lines through the data points.

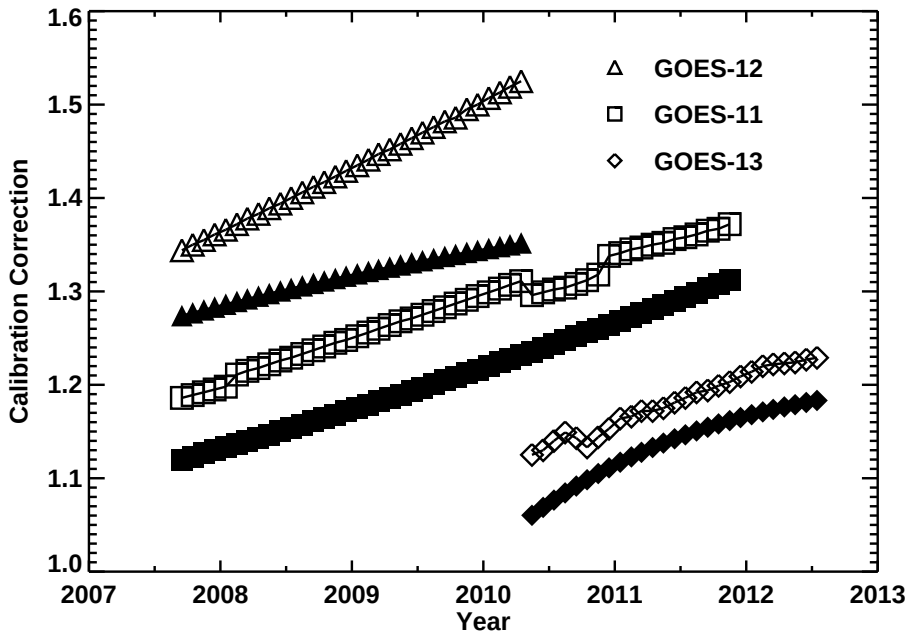

Figure 4: Calibration correction factors for GOES–11, GOES–12, and GOES–13. Open symbols represent the operational post-launch calibration published by NOAA. Filled symbols have been generated from the sensor response trends developed from the current lunar calibration analysis.

predictions, and the tools developed for GOES were readily adapted. However, the aforementioned limitations in predicting the spacecraft positions by orbit propagation also apply here. About 15 Moon images per year were found in the MSG archives. Further refinements of the Moon prediction algorithm potentially could utilize the orbital elements provided by the satellite operator, the European Organisation for the Exploitation of Meteorological Satellites (EUMETSAT).

The majority of this work on SEVIRI was conducted during a 2-week period as a Visiting Scientist by the PI at EUMETSAT in Darmstadt, Germany. This visit was sponsored by EUMETSAT, and the SEVIRI lunar calibration results will be presented at the 2012 EUMETSAT Meteorological Satellite Conference, to be held 3–7 September 2012 in Sopot, Poland.

Images of the Moon can be found only in SEVIRI level–1.0 data, since all off-Earth pixels are nulled during processing to level–1.5. But the scan line timestamps and other needed spacecraft parameters are contained in the level–1.5 headers, thus merging the two datasets was required.

Results for the SEVIRI solar channels at 0.6 μm and 0.8 μm are shown in Figure 5, where the comparisons of measured to modeled lunar irradiances are given as ratios similarly to the GOES series. The temporal trends of these time series show the SEVIRI sensors' response is comparatively stable. In each case, the linear form $a_0 + a_1(t - t_0)$ was deemed suitable for the fitted temporal functions. The series start dates and fit parameters are given in Table 3.

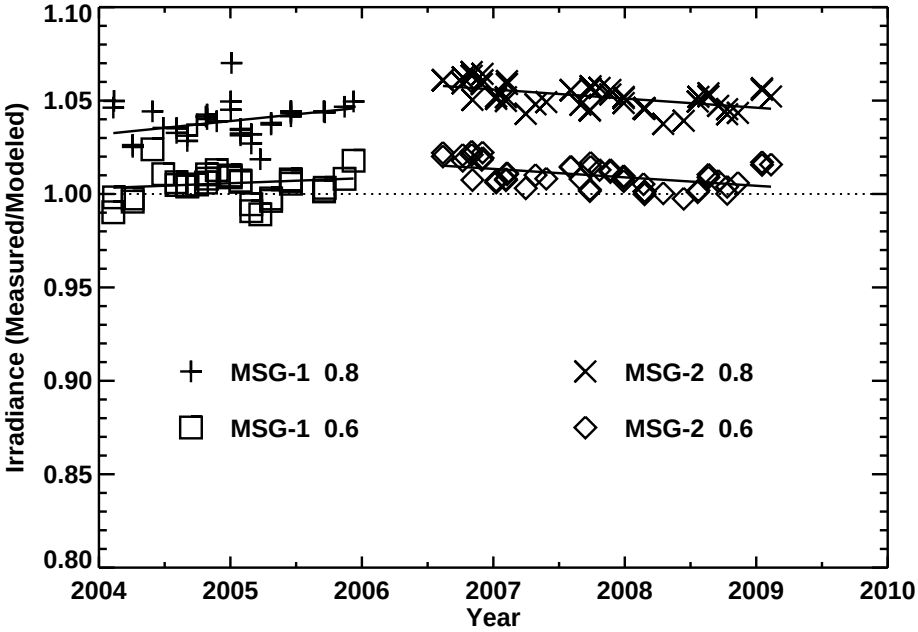

Figure 5: Time series of lunar calibration results for Meteosat Second Generation 1 and 2, given as ratios of measured lunar irradiance to USGS model outputs. Fitted trend analysis results are shown as solid lines through the data points.

Table 3: Sensor response trend analysis results

Satellite, Channel	Series Start Date (t_0)	Fit Parameters	
		a_0	a_1
MSG–1 0.6	2004–02–09	1.003	7.359E-6
MSG–1 0.8	2004–02–09	1.033	1.983E-5
MSG–2 0.6	2006–08–13	1.019	-1.891E-5
MSG–2 0.8	2006–08–13	1.061	-1.780E-5

5 AVHRR — Analysis and Assessment

The Moon periodically appears in the space view (SV) sector of routine AVHRR scans, occasionally resulting in lunar disk image captures. The SV pixels are contained in standard Global Area Coverage (GAC) data products (this was not known at the time of writing this project proposal). Sample NOAA–16 GAC data with Moon captures were obtained from CLASS, and the SV region was extracted using software routines provided by Fangfang Yu at NOAA. These data were studied in detail for potential application of lunar calibration analysis. Figure 6 shows some sample AVHRR SV Moon images and typical content.

The mean angular diameter of the Moon from LEO is about 9.04 milliradians (mrad). The AVHRR SV sector is 10 pixels wide, with a pixel angular separation ∼0.95 mrad. Thus capturing the entire lunar disk within the SV field, as required for lunar calibration, has a relatively low probability. Most of the sample NOAA–16 Moon images were found to be clipped on an edge, as seen in the top image of Figure 6. The down-track size of the lunar disk image in the SV data is ∼60 pixels. The

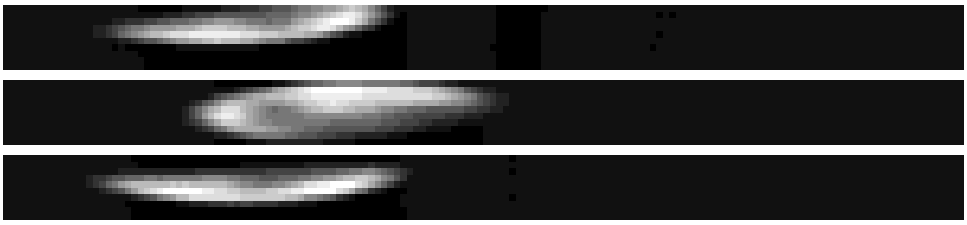

Figure 6: Sample AVHRR space view Moon images from the NOAA–16 satellite. Elongation due to oversampling is about 8:1. Top: image acquired 2001–11–24; the lunar disk is clipped along an edge. Center: image acquired 2002–02–23; the lunar disk is fully within SV sector limits, but an insufficient number of space-viewing pixels are available to evaluate the background level for each scan line. Bottom: a usable image acquired 2002-12-12.

AVHRR pixel IFOV is 1.4 mrad, thus the Moon is oversampled by a factor of ∼9.3 in the down-track direction (this measurement-based approach automatically accounts for the GAC down-track subsampling). Given the 1.4 mrad IFOV, the along-scan angular separation of 0.95 mrad, and the GAC data processing that averages 4 out of every 5 pixels along the scan line, oversampling in the along-scan direction is 1.179. Thus total oversampling is 10.96.

The AVHRR instruments utilize the space view sector (and the wider "clamp view" sector) to set the sensor bias offset, or background "space clamp" level, to typically 39–40 DN. This clamping mechanism is an integral part of the instrument — clamping is done automatically by on-board electronics and data processing, and the system presumes the space view sector always views dark space. When the Moon intrudes into the space view, the clamping mechanism drives the background level low in attempting to compensate for the higher radiance scene. This response is buffered with a time constant on the order of several seconds, and varies with the brightness of the cross-section of the Moon that has been viewed. After the Moon exits the space view, the clamp level exhibits an oscillating "ring-down" that lasts several tens of seconds before a constant level is restored. These effects are seen in Figure 7 for the 27 December 2002 data, where the image display has been stretched to reveal the background response. Since the Moon only partially fills the 10-pixel wide SV field in this image, the remaining pixels (those that actually view dark space) exhibit the space clamp response, as shown in the accompanying plot. Under these circumstances, the clamp level can be determined (within some uncertainty) for each scan line from the true space-viewing pixels, and subtracted line-by-line from the image data to give effectively zero response to zero radiance. This nulling process is a requirement to obtain lunar irradiance measurements from AVHRR images. Example results are shown in the second plot in Figure 7, where subtraction of the space clamp level was applied to a section of pixels approximately centered on the Moon's disk.

For NOAA–16, six SV Moon captures from 2001–05–30 to 2003–04–10 were found to have image characteristics favorable for lunar irradiance measurements, i.e. the lunar disk was entirely contained within the SV region, and at least one pixel of pure space-view was available to define the background level. On-moon pixel selection and summation to lunar irradiance were done similarly to the geostationary images (§4.1). Conversion of AVHRR pixel values to radiance followed the *NOAA KLM User's Guide* Section 7.1, and utilized the pre-launch radiance calibration coefficients and parameters provided in Appendix D.2 of that document:

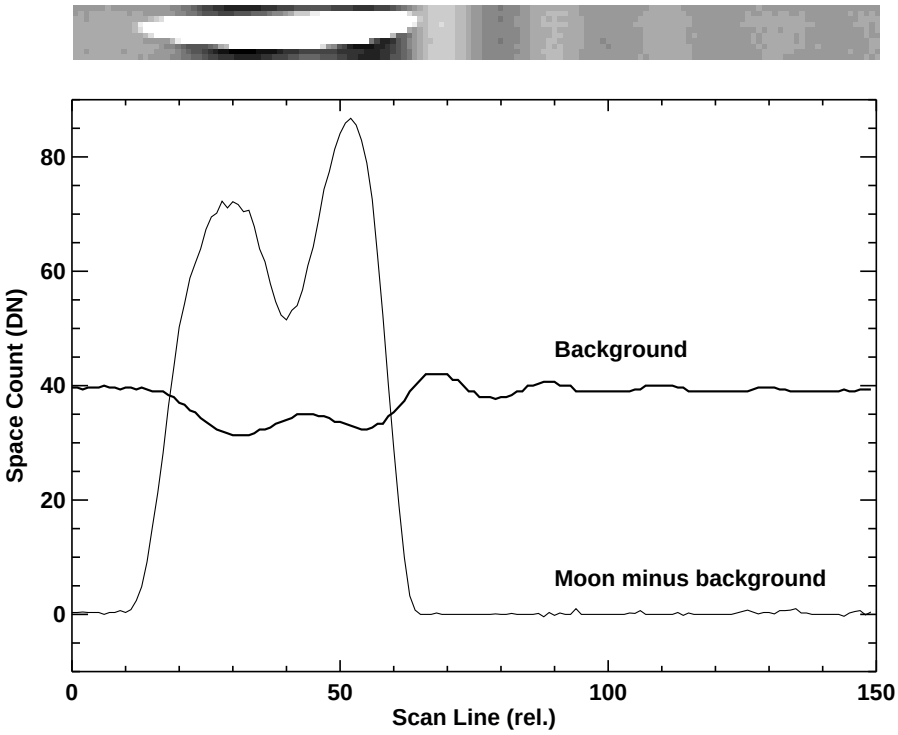

Figure 7: NOAA–16 AVHRR space view Moon image acquired 2002–12–12, with stretch applied to show the varying background level. The plots show sections of image pixels, as explained in the text.

	Center Wavelength (nm)	Radiance Calibration slope	Radiance Calibration intercept	Solar Flux (W/m^2)	Equivalent Width (nm)
Channel 1	632	0.0523	-2.016	133.2	81.0
Channel 2	843	0.0513	-1.943	243.1	235.

This operational radiance conversion presumes the background level of the image pixels is set to the space clamp level, typically 39–40 counts. After subtracting the actual (varying) clamp level from the image data, a constant value equal to (−intercept/slope) was added to all pixels prior to the radiance conversion computations.

The NOAA–16 lunar calibration results are shown in Figure 8, presented as the (relative) discrepancy δ in percent between the measured and modeled irradiance:

$$\delta = \left(\frac{\text{measured}}{\text{model}} - 1\right) \times 100\% \tag{3}$$

These AVHRR results are not conclusive, as there are still significant uncertainties in several critical factors, such as:

- the space background level, which varies by scan line
- the pixel solid angle, which depends on the IFOV shape
- oversampling, which currently relies on measurements of the Moon images.

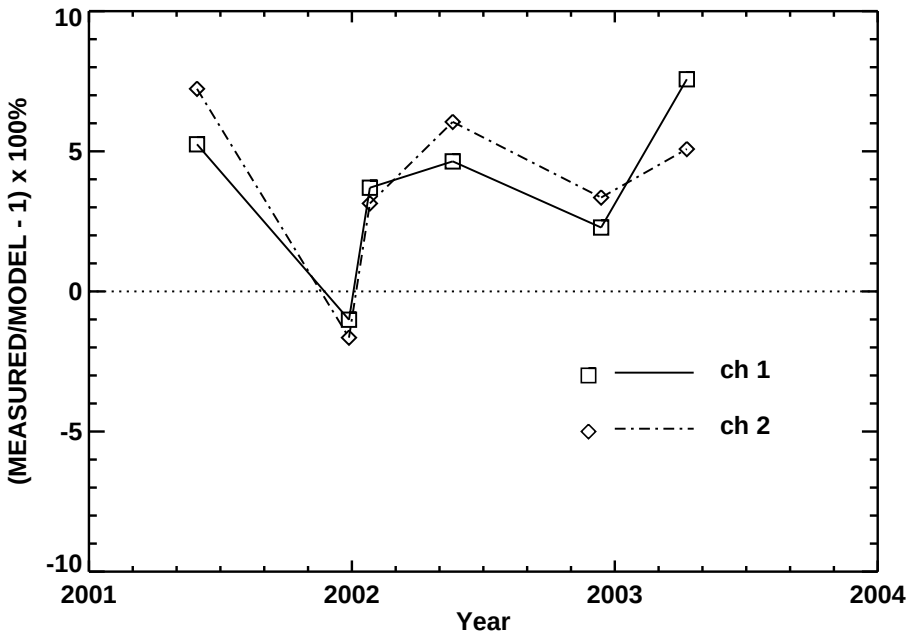

Figure 8: Time series of lunar calibration results for AVHRR on NOAA–16, given as the percent discrepancy between measured and modeled lunar irradiance (Equation 3.)

Evaluation of these uncertainties is a project second-year task. However, the nature of these AVHRR images of the Moon, particularly the automatic clamp response to lunar radiance "contamination", may lead to the determination that AVHRR SV images are not suitable for lunar calibration analysis.

6 Planned Year–2 Activities

The Year–2 tasks of this project primarily involve error assessments, to be conducted in the context of quantitative determinations of the calibration stability and inter-instrument biases of the imagers used in this study. Sources of uncertainty will be assessed for all aspects of the lunar calibration analysis, and error evaluations for the instrument calibration corrections and cross-comparisons will be generated and reported. Specific focus areas for this assessment will include:

- precision of the lunar irradiance measurements from images, including sensitivity to on-Moon pixel selection, and uncertainties in fundamental measurement parameters such as oversampling and the pixel angular size (solid angle);
- radiometric response variations among the multiple detectors of each imager;
- shorter-term stability of the imagers' radiometric response, assessed by cross-comparison of lunar images acquired at similar view geometries;
- variances in the temporal response parameters derived from the trend fits, and propagation of these uncertainties to the instrument cross-comparisons.

As an additional accuracy assessment, comparisons will be made between this and other methods for geostationary imager visible channel calibration, such as vicarious techniques using deep convective clouds as targets.

The final project task, to be completed in Year 2, is preparation and delivery to NOAA–NCDC of a technical report detailing the results of this study. The intent of this report is to provide a reliable calibration assessment for the instruments examined here, to be used by other CDR Program researchers for application to the data products of these instruments in the development of CDRs.

The project budget profile has largely adhered to the original proposal, with the exception that the trip to the NOAA Center for Satellite Applications and Research in Camp Springs, MD, was not necessary. The duration of this project is approximately two years, with the completion date of 30 September 2013 expected to be met.